

Published in final edited form as:

Nat Med. ; 17(9): 1121–1127. doi:10.1038/nm.2421.

Peroxisome proliferation-related ROS control sets melanocortin tone and feeding in diet-induced obesity

Sabrina Diano^{1,2,3,4}, Zhong-Wu Liu^{1,3}, Jin Kwoan Jeong^{1,2}, Marcelo O. Dietrich^{1,3,5}, Hai-Bin Ruan^{1,3}, Esther Kim⁶, Shigetomo Suyama^{1,3}, Kaitlin Kelly^{1,2}, Erika Gyengesi^{1,2}, Jack L. Arbiser⁷, Denise D. Belsham⁸, David A. Sarruf⁹, Michael W. Schwartz⁹, Anton M. Bennett^{1,3,10}, Marya Shanabrough^{1,3}, Charles V. Mobbs⁵, Xiaoyong Yang^{1,3}, Xiao-Bing Gao^{1,2,3}, and Tamas L. Horvath^{1,2,3,4}

¹Program in Integrative Cell Signaling and Neurobiology of Metabolism, Yale University School of Medicine, New Haven CT 06520

²Department of Ob/Gyn, Yale University School of Medicine, New Haven CT 06520

³Department of Comparative Medicine, Yale University School of Medicine, New Haven CT 06520

⁴Department of Neurobiology, Yale University School of Medicine, New Haven CT 06520

⁵Department of Biochemistry, Universidade Federal do Rio Grande do Sul, Porto Alegre RS 90035, Brazil

⁶Departments of Neuroscience and Geriatrics, Friedman Brain Institute, Mount Sinai School of Medicine, New York, NY 10029

⁷Department of Dermatology, Emory University School of Medicine, Winship Cancer Institute, Atlanta VA Medical Center, Atlanta, Georgia 30322, USA

⁸Departments of Physiology, Obstetrics and Gynaecology and Medicine, University of Toronto and Division of Cellular and Molecular Biology, Toronto General Hospital Research Institute, University Health Network, Toronto, ON, Canada M5S 1A8

⁹Diabetes and Obesity Center of Excellence, and Department of Medicine, University of Washington, Seattle, Washington, USA

¹⁰Department of Pharmacology, Yale University School of Medicine, New Haven CT 06520

Abstract

Roles for hypothalamic reactive oxygen species (ROS) in the modulation of circuit activity of the melanocortin system were proposed^{1,2}. Here we show that suppression of ROS diminished pro-opiomelanocortin (POMC) cell activation and promoted the activity of neuropeptide Y- (NPY)/agouti related peptide- (AgRP) neurons and feeding, whereas ROS activated POMC neurons and reduced feeding. ROS in POMC neurons were positively correlated with leptin levels in lean and *ob/ob* animals a relationship diminished in diet-induced obese (DIO) mice. High fat feeding resulted hypothalamic proliferation of peroxisomes and elevated PPAR γ mRNA levels.

Correspondence: sabrina.diano@yale.edu or tamas.horvath@yale.edu.

Author contribution: S.D. and T.L.H. developed the conceptual framework of the study, designed the experiments, conducted studies, analyzed data and wrote the paper. Z.-W. L., J.K.J., M.O.D., H.-B. R., E.K., S.S., K. K., E.G., D.A.S., M.S. conducted experiments. J.L.A. initiated studies with honokiol and provided reagents. C.V.M. designed and supervised in vitro cell signaling studies. M.W.S. designed studies on PPAR γ knockout mice. D.D.B. provided POMC and AgRP cell cultures and helped design experiments. A.M.B. provided reagents and advised on signaling aspects of the work. X.Y. and X.-B. G. supervised experiments and analyzed data.

Peroxisome proliferation in POMC neurons by the PPAR γ agonist, rosiglitazone, decreased ROS levels and increased food intake in lean mice on high fat diet. Suppression of peroxisome proliferation in the hypothalamus by the PPAR antagonist, GW9662, increased ROS and c-fos expression in POMC neurons, reversed high fat feeding-triggered elevated NPY/AgRP and low POMC neuronal firing, and, resulted in decreased feeding of DIO mice. Finally, central administration of ROS alone increased c-fos and pStat3 expression in POMC neurons and reduced feeding of DIO animals. These observations unmask a previously unknown hypothalamic cellular event associated with peroxisomes and ROS in the central regulation of energy metabolism in states of leptin resistance.

Much has been learned about the control of feeding behavior and of its neuronal substrate in the hypothalamus, the melanocortin system^{3,4,5,6}. One of the remaining enigmas is the neurobiological substrate of leptin resistance, a mechanism that entails the inability of increased leptin levels to promote a decreased feeding and body weight in diet-induced obese subjects⁷. Many have argued that leptin resistance is the consequence of impaired activation of anorexigenic POMC neurons by elevated leptin levels during obesity, and that this mechanism involves altered intracellular signaling cascades, including activation of Socs 3⁸. However, there is no conclusive neurobiological proof for impaired synaptic transmission in the melanocortin system in diet-induced obese animals^{9,10}. Indeed, several, neurobiologically relevant components of the melanocortin system do not exhibit a clear leptin resistance^{9,11}. Thus, the underlying cause for the impaired correlation between elevating leptin levels, POMC neuronal activity and feeding during diet-induced obesity remains elusive.

We observed that central scavenging of ROS is permissive of AgRP neuronal firing and promotion of feeding, while activity of POMC neurons and satiety is associated with increased intracellular ROS levels^{1,2}. These observations on circuit function regulated by ROS^{1,2} together with the reported effect of hypothalamic ROS in glucose- and lipid-sensing^{12,13} made us explore whether regulation of ROS plays a role in the development of impaired melanocortin tone in diet-induced obesity.

First, we analyzed the effect of a ROS scavenger on POMC neuronal activations and feeding in wild type animals (Fig. 1). We observed that intracerebroventricular (icv.) administration of the ROS scavenger, honokiol,¹⁴ resulted in significantly elevated (67.00%±8.02 SEM vs. 14.33%±6.29SEM; P<0.01) c-fos expression in NPY/AgRP and significantly neurons lower (16.54%±7.33SEM vs. 57.01%±4.85SEM, P<0.01) c-fos expression in POMC neurons compared to vehicle treated controls (Fig. 1a, b). The same treatment caused elevated food intake during the light cycle compared to vehicle controls (1h: 0.17g±0.05SEM vs. 0.01g±0.01SEM; 2h: 0.21g±0.04SEM vs. 0.01g±0.01SEM; 4h: 0.31g±0.08SEM vs. 0.06g±0.04SEM; 8h: 0.46g±0.11SEM vs. 0.1g±0.08SEM; P<0.05) (Fig. 1c). These observations are in line with our earlier findings¹, and, they revealed that suppression of ROS inhibits POMC neuronal activity as assessed by c-fos expression.

Next, we tested the effect of promotion of ROS generation on POMC neuronal activity *ex vivo* and feeding behavior *in vivo*. We conducted patch-clamp whole cell electrophysiological recordings in slice preparations from POMC-GFP mice with and without H₂O₂ application. 1 μ M H₂O₂ depolarized POMC neurons (Fig. 1d) and increased the firing rate of these cells (Fig. 1d). In line with these neurobiological effect in the arcuate nucleus, i.c.v. injection of 5 μ M H₂O₂ in 2 μ l caused decreased (P<0.01) feeding of mice after an overnight fast compared to vehicle-injected controls (Fig. 1e). This effect of H₂O₂ on promotion of decreased feeding is in line with the effect of ROS in glucose sensing and experimental hypertriglyceridemia and.^{12,13} Taken together these observations provide

evidence that ROS can be an acute regulator of POMC neuronal activity and that exogenous ROS administered to the brain can promote satiety in lean mice.

We next analyzed ROS levels in POMC cells using DHE from animals with normal metabolism (fed and fasted wild type mice) and from animals with impaired POMC neuronal activity (*ob/ob* and diet-induced obese (DIO) mice). We found the lowest level of DHE in POMC neurons of *ob/ob* mice (4.96 ± 0.23 SEM fluorescent particles per $10 \mu\text{m}^2$ of cytosol) and wild type mice that were fasted overnight (5.16 ± 0.48 SEM) (Fig. 1f, g). On the other hand, 48 h of leptin treatment¹⁰ of *ob/ob* mice resulted in elevation in DHE levels in POMC neurons compared to PBS-treated controls (16.25 ± 1.15 SEM vs. 7.5 ± 1.32 SEM fluorescent particles in $10 \mu\text{m}^2$ cytosol; $P < 0.05$). DHE levels were significantly ($P < 0.001$) higher in fed wild type animals (14.79 ± 0.83 SEM) and in DIO mice (16.61 ± 0.98 SEM) (Fig. 1f, g) compared to fasted wild type and untreated *ob/ob* values. However, there was no statistically significant difference between POMC DHE levels between fed and DIO mice (Fig. 1f, g). The lack of difference in POMC ROS levels between fed (lean) and DIO animals was associated with almost 3 fold higher levels of circulating leptin in DIO animals compared to lean fed mice (Fig. 1h). Thus, while there is a positive correlation between circulating leptin levels and ROS levels in POMC neurons of fasted and *ob/ob* animals, in DIO animals, substantially higher levels of circulating leptin had no proportional increase in ROS levels in POMC neurons (Fig. 1g, h).

The dissociation of elevated leptin levels from increased POMC ROS content in DIO mice could involve multiple mechanisms, including a putative role for mitochondrial uncoupling protein 2 (UCP2).^{1,15} We noted the presence of peroxisomes in POMC neurons. Peroxisomes are intracellular organelles involved with non-ATP generating lipid beta oxidation and control of ROS¹⁶. We evaluated the number of mitochondria and peroxisomes in POMC neurons of *ob/ob*, fasted lean, fed lean and DIO animals. We found the lowest number of mitochondria (0.8 ± 0.06 SEM mitochondria per $1 \mu\text{m}^2$ cytosol) and peroxisomes (0 peroxisome per $1 \mu\text{m}^2$ cytosol) in the cytosol of POMC in *ob/ob* animals (Fig. 2a–c). Lean fed mice had higher mitochondria number (2.19 ± 0.27 SEM) compared to fasted (0.98 ± 0.13 SEM) and *ob/ob* animals (Fig. 2b), but peroxisome numbers were not different in fed (0.18 ± 0.04 SEM) and fasted mice (0.14 ± 0.01 SEM) (Fig. 2c). While mitochondria number was not different in POMC neurons of DIO mice (2.3 ± 0.42 SEM) from that of fed animals (Fig. 2b), peroxisome counts were almost 3 fold higher in POMC neurons of DIO mice (0.39 ± 0.04 SEM) compared to the values of lean fed animals (Fig. 2c). Through analysis of 50 POMC neurons (10 cells analyzed per animal; $n=5$)¹⁷ peroxisomes were not found in POMC neurons of *db/db* mice (Supplementary Fig. 1 online). We also analyzed peroxisome number in NPY/AgRP neurons. We found that peroxisome number was significantly higher in AgRP neurons of DIO mice compared to lean values (Supplementary Fig. 2 online). Taken together these observations suggest that peroxisomes may render melanocortin neurons less active in DIO animals decreasing the ability of elevated leptin to promote POMC neuronal activity and satiety.

Proliferation of peroxisomes is governed, in part, by nuclear receptors, such as peroxisome proliferating receptor gamma (PPAR γ)¹⁸. PPAR γ was associated with brain inflammation, gliosis¹⁹ and ROS control²⁰ mechanisms that are characteristic of the arcuate nucleus of DIO animals (present study and ^{9,21}). PPAR γ was detected in the brain²² and in neurons of the arcuate nucleus²³. We analyzed transcript levels in the hypothalamus of PPAR α , δ , and γ and some of their putative target genes. PPAR γ mRNA was several fold higher in the hypothalamus compared to PPAR α or δ mRNA (Fig. 2d). In DIO mice, hypothalamic transcripts of PPAR γ but not PPAR α or δ were up-regulated compared to lean controls (Fig. 2e). DIO hypothalamus also showed elevated liver X receptor alpha (LXR α) and glucokinase transcript levels (Fig. 2e). This constellation of transcript inductions in DIO

mice is in line with both increased carbohydrate and lipid metabolism in the hypothalamus in response to high fat feeding and with processes uncovered in the liver²⁴.

Next we analyzed PPAR γ transcript levels in POMC and AgRP neuronal cell lines,²⁵. PPAR γ transcripts were identified in both neuronal cultures (Fig. 2f for POMC cultures; data not shown for NPY cultures). Treatment of the cultures with 10 μ M of the PPAR γ agonist, pioglitazone (Sigma), for 24 hrs resulted in elevated expression of the PPAR γ target gene²⁶, glycerol-3-phosphate dehydrogenase 1 (Gpd1) in POMC neurons (Fig. 2g), and expression of mRNA encoding fatty acid binding protein 4 (Fabp4) and perilipin 2 (Plin2) in NPY neurons (Fig. 2h, i). Thus, high fat feeding-inducible hypothalamic PPAR γ is expressed in key neurons of the melanocortin system, and, it can be activated by selective agonists.

In *ob/ob* hypothalamus, it was PPAR δ mRNA that was elevated together with transcripts classically characteristic of pre-adipocytes such as, cell death-inducing DNA fragmentation factor alpha-like effector A (CIDEA)²⁷ and adipose differentiation-related protein (ADFP or adipophilin) (Fig. 2j)²⁸. Thus, obesity in *ob/ob* animals has differential cellular pressure on hypothalamic neurons compared to DIO animals.

Next we tested whether chemical agonists and antagonists of PPAR γ ²⁹ may impact peroxisome number, ROS levels and feeding in lean and DIO mice. We analyzed animals (lean and DIO mice) while on high fat diet, because previous studies,³⁰ as well as the present study (data not shown) revealed no effect of PPAR γ agonists or antagonists on feeding of animals on normal chow. We i.c.v. injected lean mice after 5 days on HFD with PPAR γ agonist, rosiglitazone, twice a day for 7 days and DIO mice with 0.5 μ g of the PPAR γ antagonist, GW9662 (Sigma–Aldrich Corporation, St. Louis, MO, USA) twice a day for 7 days. We i.c.v. injected control animals for both groups with equivalent volume of the diluent. In similar cohorts of animals, we injected DHE in the last day of the treatment to analyze ROS levels in POMC neurons. Seven day i.c.v. rosiglitazone treatment of lean mice resulted in significantly elevated peroxisome number in POMC neurons compared to controls (Rosi: 0.41+0.05SEM vs. vehicle: 0.15+0.02SEM; P<0.05), which was accompanied by decreased appearance of ROS in these neurons (Rosi: 9.03 \pm 0.26SEM; vehicle: 17.55 \pm 0.4SEM; P<0.05), and increased daily food intake (4.28g+0.14SEM vs. 3.43g+0.18SEM; P<0.05) (Fig. 3a–g). In contrast, 7 day treatment of DIO mice with the PPAR γ antagonist, GW9662, resulted in lower number of peroxisomes in POMC neurons compared to controls (GW9662: 0.17+0.02SEM; vehicle: 0.4+0.05SEM; P<0.05), with elevated DHE levels (GW9662: 27.45 \pm 2.92SEM; vehicle: 18.31 \pm 0.66SEM; P<0.05) and lower daily food intake (GW9662: 2.29g+0.1SEM, vehicle: 2.92g \pm 0.11SEM; P<0.05) (Fig. 3a–g). These observations are consistent with two recent reports showing that interference with neuronal PPAR γ signaling has no detectable phenotype on standard chow, but attenuates DIO.^{31,32}

To further test the relationship PPAR γ and peroxisomes, we analyzed the expression of a key peroxisomal enzyme, catalase, in hypothalami of neuron-specific PPAR γ knockout mice³¹ and wild type littermates. After 2 weeks on high fat diet, wild type animals exhibited significantly higher number of catalase-immunopositive arcuate nucleus cells compared to PPAR γ knockout mice (51.75+5.75 cells/0.0025mm³ of arcuate nucleus versus 12.75+3.75 cells/0.0025mm³ of arcuate nucleus; P<0.05; Supplemental Fig. 3 online). This data corroborates a role for PPAR γ in peroxisome proliferation in the hypothalamus.

To test whether interference with PPAR γ activity affects neurobiological correlates of feeding regulation, first we analyzed c-fos expression in POMC neurons of vehicle-, rosiglitazone- and GW9662-treated female mice on high fat diet. While rosiglitazone did not

affect the number of c-fos expressing POMC neurons, GW9662 treatment resulted in a significant ($P < 0.05$) induction of c-fos in melanocortin cells compared to DIO control values (Fig. 3h, i; Supplementary Fig. 4 online).

Because GW9662 induced c-fos expression in POMC neurons, and because peroxisome number and PPAR γ signaling were induced also in NPY neurons, we next analyzed electric activity of NPY/AgRP and POMC neurons in GFP-NPY and GFP POMC DIO mice with or without GW9662 treatment. Firing rate of NPY/AgRP and POMC neurons were measured on slices taken at 10:00AM from GW9662 or vehicle-treated DIO mice. This time point of the day represents relative satiety with high POMC and low NPY/AgRP neuronal firing of standard chow fed mice.^{14,32} In contrast to chow fed mice, in vehicle-treated DIO animals, analysis of action potential frequency at 10:00AM revealed elevated NPY/AgRP neuronal firing and low POMC firing (Fig. 4a, b). The level of NPY/AgRP neuronal firing in fed DIO mice was not dissimilar from the firing frequency recorded in these neurons during fasting.³³ The low firing of POMC neurons at the time of relative satiety in DIO mice is consistent with the measured lower α -melanocyte stimulating hormone (α -MSH) release by hypothalamic explants of the DIO mice.¹⁵ Of note, i.c.v. GW9662 treatment significantly ($P < 0.05$) reversed this DIO-induced firing alteration of the melanocortin system, whereby NPY/AgRP neurons reduced their firing rate and POMC neurons increased action potential generation (Fig. 4a, b). In DIO animals, very few NPY/AgRP neurons were silent, but this number was elevated after GW9662 treatment (Fig. 4c). On the other hand, while more than half of the POMC neurons were silent (not firing at all) in vehicle-treated DIO mice, this population was lower after GW9662 treatment (Fig. 4d). Thus, GW9662 reversed firing of both NPY/AgRP and POMC neurons in DIO animals to resemble the firing rates of these cells in lean animals at a time of satiety on normal chow.^{15,33}

ROS was elevated by GW9662 treatment and readily enhanced POMC neuronal firing (Fig. 1). To test whether ROS may be a mediator of the effects of PPAR γ , we next analyzed the effect of rosiglitazone and GW9662 in animals on high fat diet with and without i.c.v. H202 and honokiol administration, respectively. We found that 5 day treatment-induced changes in feeding of high fat fed animals by rosiglitazone or GW9662 were diminished by subsequent 2 day parallel i.c.v. administration of H202 or honokiol, respectively (Fig. 4e, f). Thus, alteration of PPAR γ signaling may exert its effect on hypothalamic regulation of feeding via ROS. To further test this, we analyzed the effect of GW9662 and rosiglitazone in UCP2 knockout mice, an animal model that had endogenously elevated hypothalamic ROS levels.¹ We found no significant effect of either GW9662 or rosiglitazone on feeding of these animals (Supplementary Fig. 5 online). The lack of effect rosiglitazone in UCP2 knockout mice is in line with inhibitory effect of ROS on rosiglitazone. GW9662 may not have been effective because there were very few peroxisomes in POMC neurons of UCP2 knockout mice (Supplementary Fig. 5 online).

To test whether ROS alone could reverse POMC function, we injected H202 i.c.v. in DIO mice. We found that i.c.v. H202 resulted in elevated c-fos expression in POMC neurons (Fig. 3h, i and Supplementary Fig. 4d online), lower feeding (Fig. 4g) and elevated pStat3 expression in response to peripheral leptin injection compared to controls (Fig. 4h). We found 3% POMC (3 out of 100 POMC perikarya from 5 animals) to contain pStat3, while in H202-treated DIO mice, 18% of POMC cells (18 out of 100 POMC perikarya from 5 animals) were immunolabeled for pStat3. These observations suggest that while ROS enhances leptin sensitivity in DIO animals, ROS' effect on feeding may be downstream from leptin signaling, a notion consistent with the electric actions of H2O2 on POMC neurons (Fig. 1). How other intracellular controllers of ROS interact to set metabolically and functionally relevant cellular ROS levels will need further studies.

Our studies established that ROS is an acute activator of POMC neuronal firing, and that in lean animals, hypothalamic ROS is positively correlated with circulating leptin level. ROS levels are controlled in hypothalamic POMC neurons of DIO animals in association with peroxisome proliferation. This novel metabolically regulated intracellular mechanism can be regulated by PPAR γ activity, which, itself is under nutritional control in the hypothalamus. Peroxisome proliferation in the hypothalamus is consistent with the origin of peroxisomes from the endoplasmic reticulum under increased metabolic pressure^{34,35} as endoplasmic reticulum stress was identified as contributor to DIO-related leptin resistance³⁶. Our results argue for endogenous ROS control during diet-induced obesity as a potential cause of functional leptin resistance manifested by lower POMC and elevated NPY/AgRP neuronal firing. In light of the deleterious effects of sustained elevated ROS levels³⁷, our study gives support to the notion that promotion of sustained satiety through the brain in diet-induced obese may increase degenerative processes².

Methods

All procedures described below have been approved by the Institutional Animal Care and Use Committee of Yale University. Mice were kept under standard laboratory conditions with free access to food and water. All experiments described below were conducted on C57Bl6 (and *ob/ob* when specified) male and female mice maintained on either NPY-GFP, POMC-GFP or UCP2 knockout mice.^{1,10} Regular diet: Purina Lab Chow #5001, Ralston Purina Corp, St. Louis, MO. HFD: Rodent Chow #D12451, Research Diets Inc., New Brunswick, NJ. HFD was fed for 12 weeks starting at 6 weeks of age. Daily food intake was assessed in individually housed mice.

Lateral ventricle cannulation

A sterile guide cannula 9 mm in length was implanted into the lateral brain ventricle (0.3 mm posterior and 1 mm lateral relative to bregma, and 3 mm below the surface of the skull). The position of the cannula was verified at the end of the experiments by dye administration before animals were killed.

Honokiol or its vehicle was administered icv. at 9:00AM and food intake was measure for the subsequent 8 hours. 2 μ l of stock solution of 37.6 mM honokiol (Wako Chemical Company, Tokyo, Japan) dissolved in 100 μ l ethanol that was further dissolved in 1ml of intralipid was injected¹⁴.

5 μ M H₂O₂ in 2 μ l saline was injected icv. of lean mice. Saline was used as vehicle. Rebound feeding after a 16h fast was analyzed. The same dose of H₂O₂ (and vehicle) was also injected icv. to DIO female mice (n=6) 3 times, the injections 8 hours apart. Daily food intake was measured before and after the treatment. In a subset of these mice, we injected intraperitoneally 3 μ g/g body weight recombinant leptin dissolved in PBS. Animals were killed 45 minutes later and processed for pStat3 (Cell Signaling Technology Inc., Danvers, MA) and POMC immunolabeling,

PPAR γ agonists (rosiglitazone; Enzo Life Sciences Inc., Farmingdale, NY, USA) and antagonist GW9662 (2-chloro-5-nitrobenzanilide) were purchased from Alexis Biochemicals and dissolved in dimethyl sulfoxide (DMSO) in saline (1:3 ratio). 0.5mg of rosiglitazone or GW9662 in 2 μ l of vehicle was injected into i.c.v. twice daily (9:00AM and 6:00 PM) for 7 days.

In sets females (n=6), after the 5th days of rosiglitazone treatment, H₂O₂ (5 μ M H₂O₂ in 2 μ l) or saline was also administered icv. to animals in association with rosiglitazone treatment at days 6 and 7. In other sets of females (n=6), after the 5th day of GW9662

treatment, honokiol or its vehicle was also administered in association with the GW9662 treatments at days 6 and 7. Daily food intake was monitored and analyzed at days 5 and 7 in all groups.

c-fos staining in NPY and POMC neurons

NPY GFP or POMC GFP and mice were treated with honokiol or vehicle and rapidly perfused 1 hour later. c-fos immunofluorescence staining was carried out as described before.¹⁷

Electrophysiology

Whole cell recording was made in POMC-GFP neurons in the arcuate nucleus (ARC) of the hypothalamus as described previously²⁴. For firing rate analysis in older DIO mice, we used extracellular recordings from GFP labeled NPY or POMC cells.

DHE

ROS levels in identified POMC GFP neurons were measured by injecting dihydroethidium (DHE) as described before.¹

Leptin treatment of ob/ob animals

Alzet 2002 mini-osmotic pumps (Alza, Palo Alto, CA) were implanted into 8 weeks old obese transgenic mice subcutaneously under anesthesia¹⁰. Pumps were filled with either PBS (control) or 420 ng/ μ l leptin (Amgen, Thousand Oaks, CA). Pumps were incubated the night before at 37°C in sterile 0.9% NaCl. Animals and food were weighted daily at midday. Animals were sacrificed at 48 hours after implantation and 3 hours after DHE injections.

Measurement of leptin

Blood levels of leptin were measured by ELISA using commercially available Leptin Elisa Kit.

Mitochondria and peroxisome counts

Animals were perfused and their brains were processed for GFP immunolabeling for electron microscopic examination as described before.¹

Cell Culture

The POMC- and AgRP-expressing hypothalamic neuronal cell lines were cultured as previously described²⁵. The culture media contained 0.5 mM glucose with or without 10 μ M pioglitazone (Sigma) for 24 hrs.

Real time PCR

RNA from hypothalamus or cultures was isolated using RNeasy Micro Kit (Qiagen) and reverse transcribed to cDNA using MultiScribe Reverse Transcriptase (Applied Biosystems). Quantitative PCR was performed with SYBR Green I Master or Probe Master using LightCycler 480 Real time PCR system (Roche).

PPAR γ NKO mice

Mice with neuron-specific PPAR γ (PPAR γ NKO) were generated as described recently.³¹ Sections from 14 week old mice with or without 2 weeks on HFD were processed for catalase immunocytochemistry.

Statistical Analysis

All data are expressed as the mean \pm sem. The means between two groups were analysed by student t-test and between more than two groups and two genotypes by two-way ANOVA followed by Bonferroni posthoc tests unless otherwise stated. Significance was taken at $p < 0.05$.

Supplementary Material

Refer to Web version on PubMed Central for supplementary material.

Acknowledgments

We thank Jerrold M Olefsky, Department of Medicine, University of California–San Diego (UCSD), San Diego, CA, USA, for generating and providing brain-specific PPAR γ knockout animals, and Bradford B. Lowell, Beth Israel Deaconess Medical Center, Boston, MA, USA for providing breeding pairs of UCP2 knockout animals. This work was supported by US National Institutes of Health (NIH) grants DK084065 (S.D), DK080000 and OD006850 (T.L.H.), and by American Diabetes Association grant 7-08-MN-25 (T.L.H.). This work was also supported by NIH grants DK089098 (X.Y.), DK072033 (C.V.M.) DK090320 (M.W.S), AR47901 and P30 AR42687 (J.L.A).

References

- Andrews Z, et al. UCP2 mediates ghrelin's action on NPY/AgRP neurons by lowering free radicals. *Nature*. 2008; 454:846–51. [PubMed: 18668043]
- Horvath TL, Andrews ZB, Diano S. Fuel Utilization by Hypothalamic Neurons: Roles for ROS. *Trends in Endocrinology and Metabolism*. 2009; 20:78–87. [PubMed: 19084428]
- Gropp E, et al. Agouti-related peptide-expressing neurons are mandatory for feeding. *Nature Neuroscience*. 2005; 8:1289–91.
- Luquet S, Perez F, Hnasko T, Palmiter R. NPY/AgRP neurons are essential for feeding in adult mice but can be ablated in neonates. *Science*. 2005; 310:683–685. [PubMed: 16254186]
- Cone RD. Studies on the physiological functions of the melanocortin system. *Endocr Rev*. 2006; 27:736–49. [PubMed: 17077189]
- Gao Q, Horvath TL. Neurobiology of feeding and energy expenditure. *Ann Rev Neurosci*. 2007; 30:367–98. [PubMed: 17506645]
- Halaas J, et al. Physiological response to long-term peripheral and central leptin infusion in lean and obese mice. *Proc Natl Acad Sci U S A*. 1997; 94:8878–83. [PubMed: 9238071]
- Bjørbaek C, Elmquist JK, Frantz JD, Shoelson SE, Flier JS. Identification of SOCS-3 as a potential mediator of central leptin resistance. *Mol Cell*. 1998; 1:619–25. [PubMed: 9660946]
- Horvath T, et al. Synaptic Input Organization of the Melanocortin System Predicts Diet-Induced Hypothalamic Reactive Gliosis and Obesity. *Proc Natl Acad Sci U S A*. 2010; 107:14875–80. [PubMed: 20679202]
- Pinto S, et al. Rapid Re-wiring of Arcuate Nucleus Feeding Circuits by Leptin. *Science*. 2004; 304:110–115. [PubMed: 15064421]
- Pal R, Sahu A. Leptin signaling in the hypothalamus during chronic central leptin infusion. *Endocrinology*. 2003; 144:3789–98. [PubMed: 12933650]
- Leloup C, et al. Mitochondrial reactive oxygen species are required for hypothalamic glucose sensing. *Diabetes*. 2006; 55:2084–90. [PubMed: 16804079]
- Benani A, et al. Role for mitochondrial reactive oxygen species in brain lipid sensing: redox regulation of food intake. *Diabetes*. 2007; 56:152–60. [PubMed: 17192477]
- Dikalov S, Losik T, Arbiser JL. Honokiol is a potent scavenger of superoxide and peroxy radicals. *Biochem Pharmacol*. 2008; 76:589–96. [PubMed: 18640101]
- Parton LE, et al. Glucose sensing by POMC neurons regulates glucose homeostasis and is impaired in obesity. *Nature*. 2007; 449:228–32. [PubMed: 17728716]
- Schrader M, Fahimi HD. Peroxisomes and oxidative stress. *Biochim Biophys Acta*. 2006; 1763:1755–66. [PubMed: 17034877]

17. Gao Q, et al. Anorexigenic estradiol mimics leptin's effect on re-wiring of melanocortin cells and Stat3 signaling in obese animals. *Nature Medicine*. 2007; 13:89–94.
18. Green S. PPAR: a mediator of peroxisome proliferator action. *Mutat Res*. 1995; 333:101–9. [PubMed: 8538617]
19. Bernardo A, Minghetti L. PPAR-gamma agonists as regulators of microglial activation and brain inflammation. *Curr Pharm Des*. 2006; 12:93–109. [PubMed: 16454728]
20. Yu X, et al. Activation of cerebral peroxisome proliferator-activated receptors gamma exerts neuroprotection by inhibiting oxidative stress following pilocarpine-induced status epilepticus. *Brain Res*. 2008; 1200:146–58. [PubMed: 18289512]
21. Thaler JP, Schwartz MW. Minireview: Inflammation and obesity pathogenesis: the hypothalamus heats up. *Endocrinology*. 2010; 151:4109–15. [PubMed: 20573720]
22. Cullingford T, et al. Distribution of mRNAs encoding the peroxisome proliferator-activated receptor alpha, beta, and gamma and the retinoid X receptor alpha, beta, and gamma in rat central nervous system. *J Neurochem*. 1998; 70:1366–75. [PubMed: 9523552]
23. Sarruf D, et al. Expression of peroxisome proliferator-activated receptor-gamma in key neuronal subsets regulating glucose metabolism and energy homeostasis. *Endocrinology*. 2009; 150:707–12. [PubMed: 18845632]
24. Kim TH, et al. Interrelationship between liver X receptor alpha, sterol regulatory element-binding protein-1c, peroxisome proliferator-activated receptor gamma, and small heterodimer partner in the transcriptional regulation of glucokinase gene expression in liver. *J Biol Chem*. 2009; 284:15071–83. [PubMed: 19366697]
25. Belsham D, et al. Ciliary neurotrophic factor recruitment of glucagon-like peptide-1 mediates neurogenesis, allowing immortalization of adult murine hypothalamic neurons. *FASEB J*. 2009; 23:4256–4265. [PubMed: 19703933]
26. Poplawski M, et al. Hypothalamic responses to fasting indicate metabolic reprogramming away from glycolysis toward lipid oxidation. *Endocrinology*. 2010; 151:5206–5217. [PubMed: 20881243]
27. Puri V, et al. Cidea is associated with lipid droplets and insulin sensitivity in humans. *Proc Natl Acad Sci U S A*. 2008; 105:7833–8. [PubMed: 18509062]
28. Heid H, et al. Adipophilin is a specific marker of lipid accumulation in diverse cell types and diseases. *Cell Tissue Res*. 1998; 294:309–21. [PubMed: 9799447]
29. Kouidhi S, et al. Peroxisome proliferator-activated receptor-gamma (PPARgamma) modulates hypothalamic Trh regulation in vivo. *Mol Cell Endocrinol*. 2010; 317:44–52. [PubMed: 19900503]
30. Festuccia W, et al. Peroxisome proliferator-activated receptor-gamma-mediated positive energy balance in the rat is associated with reduced sympathetic drive to adipose tissues and thyroid status. *Endocrinology*. 2008; 149:2121–30. [PubMed: 18218698]
31. Lu M, et al. Brain Peroxisome Proliferator-Activated Receptor Gamma Promotes Obesity and is Required for the Full Insulin-Sensitizing Effect of Thiazolidinediones. *Nat Med*. May.2011
32. Ryan K, et al. A role for central nervous system PPAR- γ in the regulation of energy balance. *Nat Med*. May.2011
33. Takahashi KA, Cone RD. Fasting induces a large leptin-dependent increase in the intrinsic action potential frequency of orexigenic arcuate nucleus neuropeptide Y/Agouti-related protein neurons. *Endocrinology* 2005. 2005; 146:1043–7.
34. Hoepfner D, et al. Contribution of the endoplasmic reticulum to peroxisome formation. *Cell*. 2005; 122:85–95. [PubMed: 16009135]
35. Tabak HF, et al. Formation of peroxisomes: present and past. *Biochim Biophys Acta*. 2006; 1763:1647–54. [PubMed: 17030445]
36. Ozcan L, et al. Endoplasmic reticulum stress plays a central role in development of leptin resistance. *Cell Metab*. 2009; 9:35–51. [PubMed: 19117545]
37. Finkel T, Holbrook NJ. Oxidants, oxidative stress and the biology of ageing. *Nature*. 2000; 408:239–47. [PubMed: 11089981]

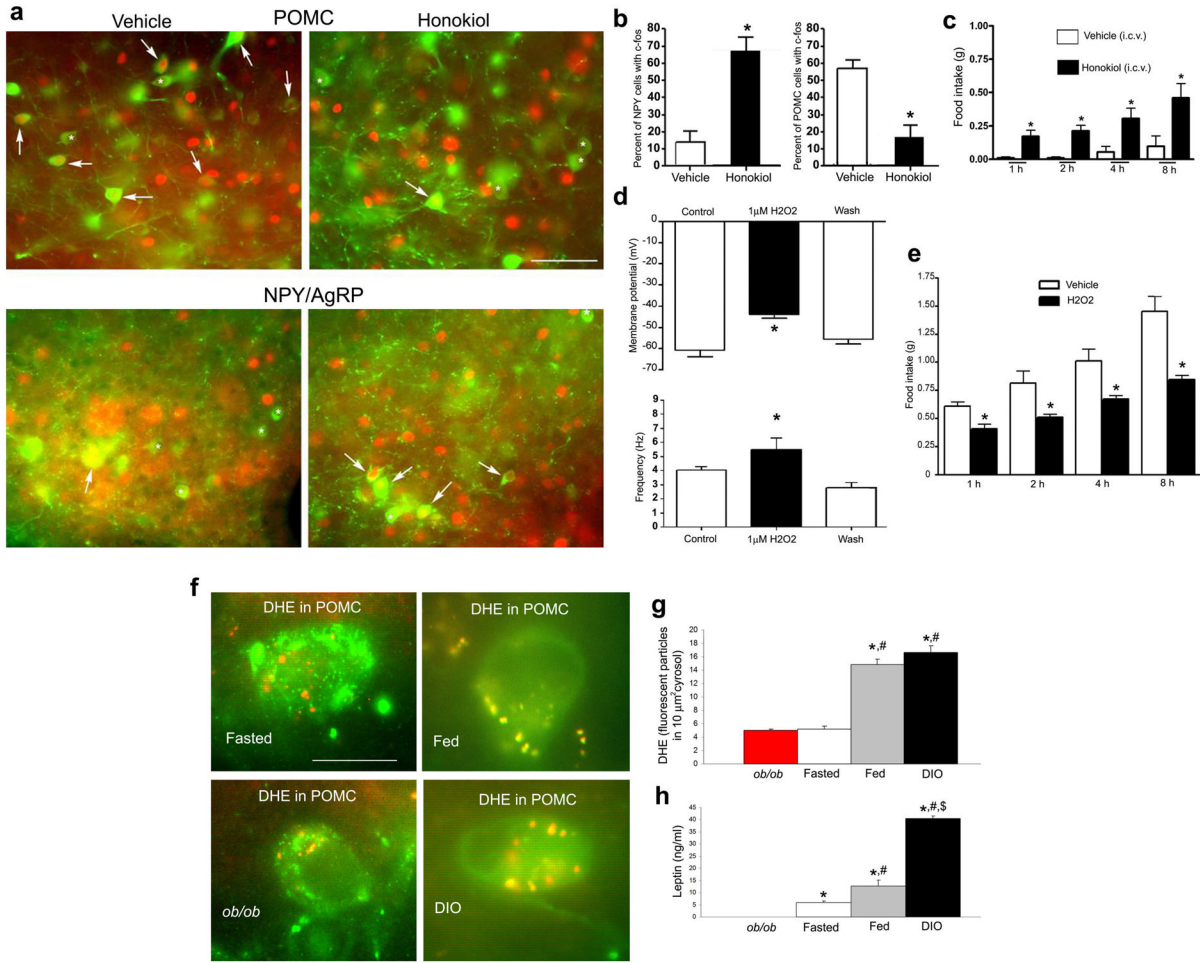


Fig. 1. Honokiol suppresses while H2O2 increases anorexigenic melanocortin tone and related feeding

a: Fluorescence double labeling for c-fos (red nuclei) and GFP (green cell bodies) shows colocalization of c-fos with GFP (white arrows) in vehicle- and honokiol-treated animals. Bar scale on upper right panel of **a** indicates 100 μm for all 4 panels.

b: Honokiol treatment elevated the percent of c-fos/NPY-GFP double labeled neurons compared to vehicle controls. Honokiol treatment decreased the percentage of c-fos/POMC-GFP double labeled cells. * indicates $P < 0.05$.

c: Food intake was significantly induced by icv. honokiol treatment. * $P < 0.05$.

d: Upper panel: H2O2 significantly (* $P < 0.05$) depolarized membrane potential of POMC-GFP neurons an event that was rapidly reversed by washout. Control values indicate firing of POMC neuron when exposed to vehicle. Lower panel: H2O2 significantly increased ($P < 0.05$) the firing frequency of arcuate nucleus POMC-GFP neurons, and event that was reversed by washout. Control values indicate firing of POMC neuron when exposed to vehicle.

e: Icv. administration of H2O2 significantly reduced food intake of mice 1h (* $P < 0.05$), 2h (* $P < 0.05$), 4h (* $P < 0.05$) and 8h (* $P < 0.05$) subsequent to injections. Control animals were injected with equivalent amount of vehicle.

f: DHE (red fluorescence) in POMC neurons (green fluorescence) of *ob/ob*, fasted lean, fed lean and diet-induced obese (DIO) mice.

g: Quantification of DHE in POMC neurons indicated the highest level of ROS production in POMC neurons of DIO and fed lean mice compared to fasted lean and *ob/ob* mice. *indicates significant ($P<0.05$) difference compared to *ob/ob* values. # indicates significant ($P<0.05$) difference compared to fasted lean values. There was no significant difference between fed and DIO values.

h: Leptin levels were not detectable in *ob/ob* mice. Leptin levels were significantly higher in fed animals compared to fasted values (#: $P<0.05$). DIO animals had leptin levels that were significantly higher compared to fed (\$: $P<0.05$) and fasted values (#: $P<0.05$). * indicates significant ($P<0.05$) difference compared to *ob/ob* values.

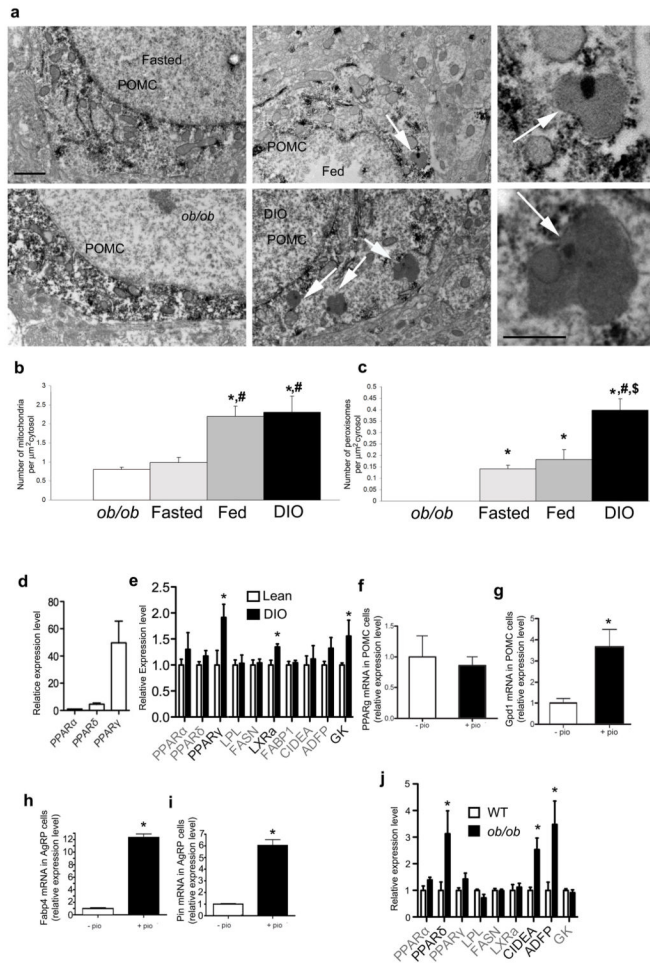


Fig. 2. Peroxisome proliferation in POMC neurons

a: Electron micrographs showing representative section of POMC-GFP perikarya in the arcuate nucleus from fasted lean (upper left panel), *ob/ob* (lower left panel), fed lean (upper middle panel) and DIO (lower middle panel). White arrows on the middle panels point to peroxisomes. The upper right and lower right panels are high power magnifications of peroxisomes from the fed and DIO panels, respectively. Bar scale on upper left panel indicate 1 μm for left and middle panels. Bar scale on lower right panel indicates 500 nm for the right panels.

b: Mitochondria number was the highest in POMC neurons of fed and DIO mice compared to fasted and *ob/ob* values. *: significantly different ($P < 0.05$) from *ob/ob* values. #: significantly ($P < 0.05$) different from fasted values.

c: Highest number of peroxisomes in POMC neurons was in DIO animals. Significantly lower numbers of peroxisomes were detected in fed and fasted animals, while no peroxisomes were detected in POMC neurons of *ob/ob* animals. *: significantly different ($P < 0.05$) from *ob/ob* values. #: significantly ($P < 0.05$) different from fasted values. \$: significantly ($P < 0.05$) different from fed values.

d: PCR analyzes of PPARα, δ and γ shows that absolute levels of PPARγ is several fold higher than transcripts of PPARα and δ in the hypothalamus.

e: Real time PCR analyzes of PPARα, δ and γ and various other gene transcripts related to PPAR signaling and cellular metabolism in DIO hypothalamus relative to lean control values. LPL: lipoprotein lipase, FASN: fatty acid synthase, LXRα: liver X receptor alpha,

FABP1: fatty acid binding protein 1, CIDEA: cell death-inducing DFFA-like effector a, ADFP/PLIN2: adipose differentiation related protein/perilipin 2, GCK: glucokinase. Results are shown as mean \pm SEM. The comparison of different groups was carried out using two-tailed unpaired Student's t-test. * indicates $P < 0.05$.

f: PPAR γ mRNA is expressed in POMC neuronal cell line mHypoA-2/28, and its relative expression level did not change after pioglitazone treatment (pio).

g: Pioglitazone induced the expression of the PPAR γ target gene, Gpd1 in the POMC-expressing hypothalamic cell line.

h: Pioglitazone induced the expression of the PPAR γ target gene, Fabp4 in the AgRP-expressing hypothalamic cell line.

i: Pioglitazone induced the expression of the PPAR γ target gene, Pin2 in the AgRP-expressing hypothalamic cell line.

j: Real time PCR analyzes of PPAR α , δ and γ and various other gene transcripts related to PPAR signaling and cellular metabolism in *ob/ob* hypothalamus relative to wild type controls. LPL: lipoprotein lipase, FASN: fatty acid synthase, LXRA: liver X receptor alpha, FABP1: fatty acid binding protein 1, CIDEA: cell death-inducing DFFA-like effector a, ADFP/PLIN2: adipose differentiation related protein/perilipin 2, GCK: glucokinase. Results are shown as mean \pm SEM. The comparison of different groups was carried out using two-tailed unpaired Student's t-test. * indicates $P < 0.05$.

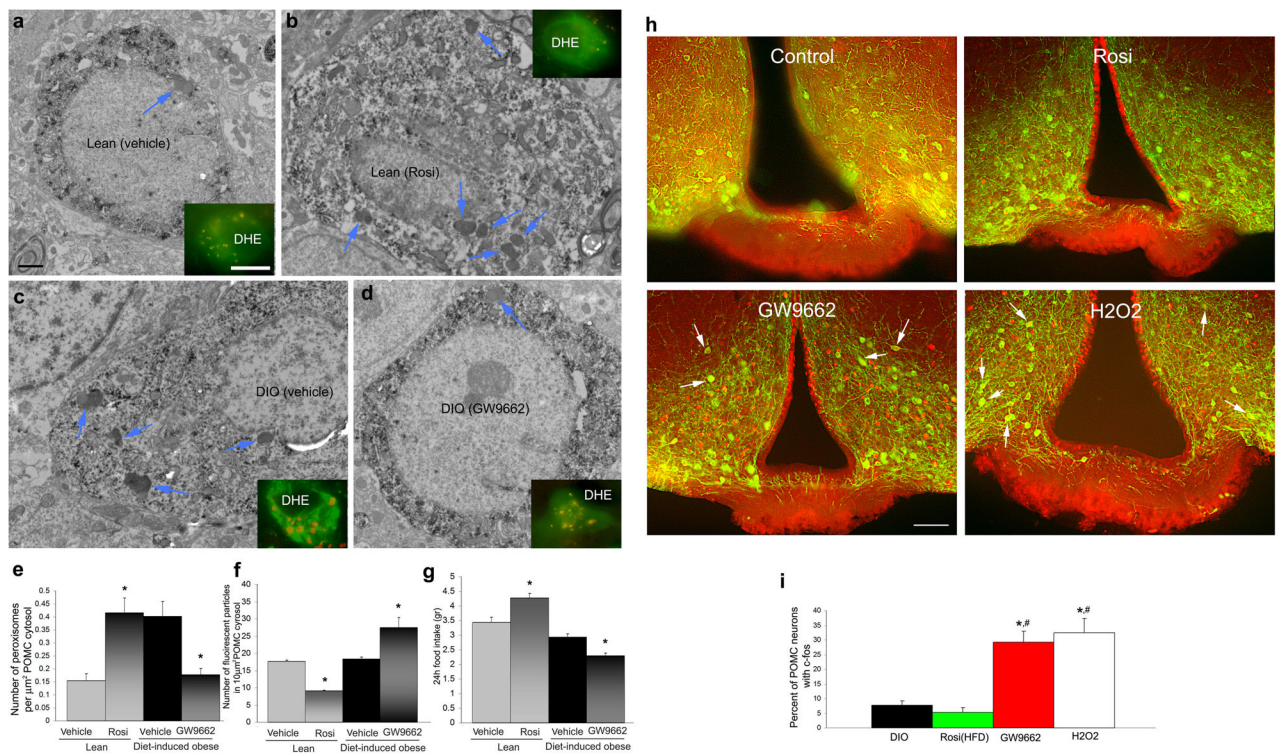


Fig. 3. Peroxisome proliferation in POMC neurons is associated with altered feeding

a-d: Electron micrographs with fluorescence inserts of POMC neurons from lean vehicle-treated (upper left panel), lean rosiglitazone-treated (upper right panel), DIO-vehicle treated (lower left panel) and DIO GW9662-treated (lower right panel) mice. On the electron micrographs, blue arrows point to peroxisomes. On the fluorescent inserts, red labeling indicated DHE in green POMC-GFP neurons. Bar scale on the upper left electron micrograph indicates 1 μm for all EM panels; bar scale on the fluorescent insert of the upper left panel indicate 10 μm for all inserts.

e: Rosiglitazone induced increase in peroxisome number in POMC neurons of lean animals on high fat diet. On the other hand, treatment of DIO mice with the PPAR γ antagonist, GW9662, decreased peroxisome number in POMC neurons. *: $P < 0.05$.

f: DHE levels were decreased in lean animals treated with rosiglitazone, while DIO animals treated with GW9662 had elevated DHE counts. *: $P < 0.05$.

g: Treatment of lean mice consuming normal chow with rosiglitazone, daily food intake of animals was significantly higher compared to vehicle-treated values. GW9662 treatment of DIO mice consuming high fat diet resulted in a decline in daily food intake. *: $P < 0.05$.

h: Double immunofluorescence labeling for c-fos (red) and POMC (green) from control DIO (upper left panel), rosiglitazone-treated (upper right panel), GW9662-treated (lower left panel) and H2O2-treated (lower right panel) high fat-fed animals. Bar scale on lower left panel represents 100 μm for all panels of **h**.

i: Bar graphs showing the percentage of c-fos immunolabeled POMC neurons in the different experimental groups. * indicates significant ($P < 0.05$) difference compared to DIO control values; # indicates significant ($P < 0.05$) differences compared to values of rosiglitazone treated animals.

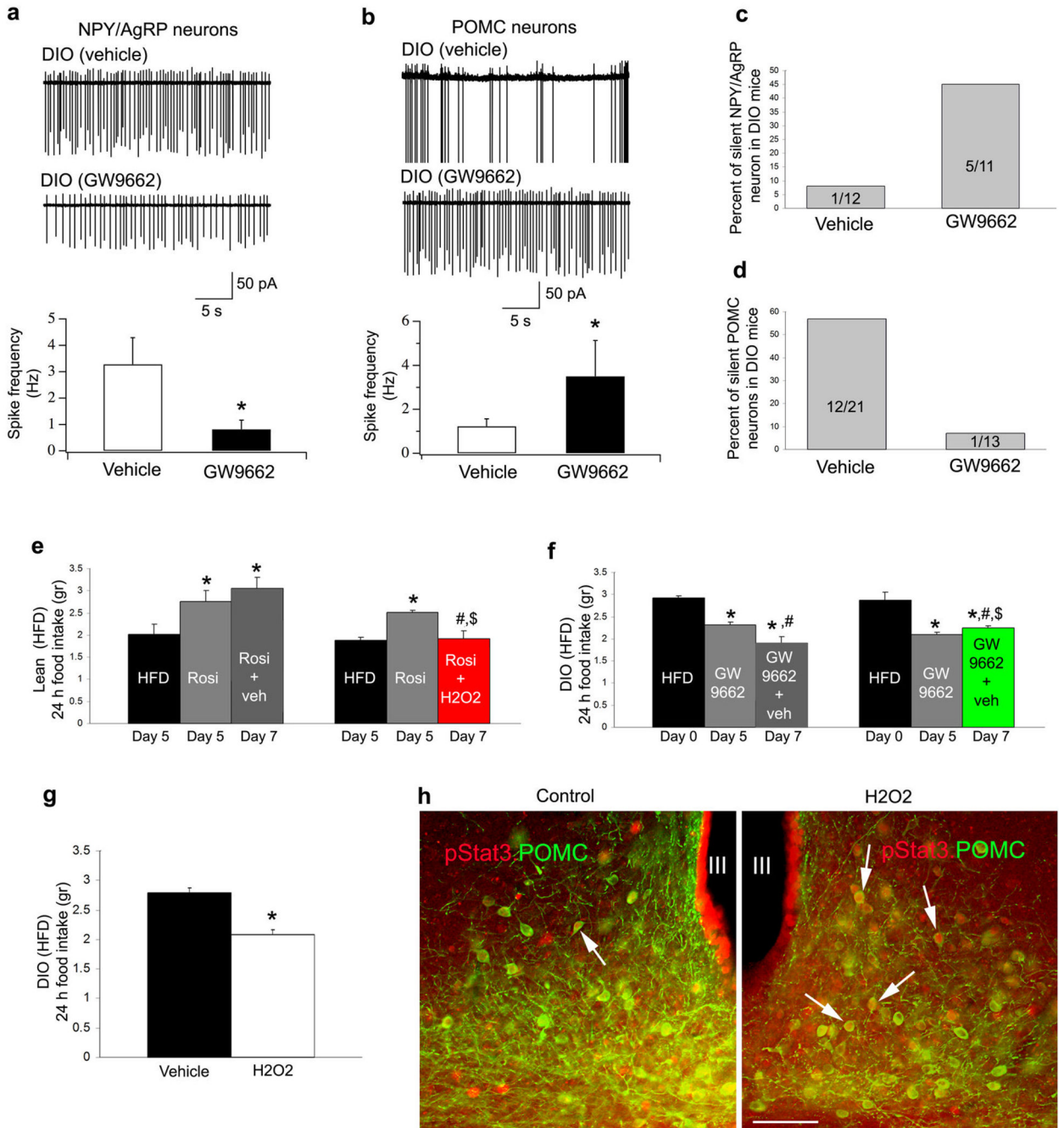


Fig. 4. GW9662 reverses DIO-triggered electric activity of the melanocortin system and ROS regulates feeding behavior in DIO animals
a: Firing rate of DIO NPY/AgRP neurons is significantly decreased (*:P<0.05) by GW9662 treatment.
b: Firing rate of DIO POMC neurons is significantly increased (*:P<0.05) by GW9662 treatment.
c: GW9662 treatment increased the percentage of silent DIO NPY/AgRP neurons.
d: GW9662 treatment decreased the percentage of silent DIO POMC neurons.
e: Rosiglitazone induces food intake in lean animals. Left column indicates daily food intake after 5 days on high fat diet. Middle column shows mean daily food intake after 5 days

treatment with rosiglitazone. Right column indicates daily food intake after 7 days rosiglitazone treatment. Red bar graph on right indicates daily food intake of animals with 7 day rosiglitazone treatment with H2O2 in the last 2 days of the 7 day treatment. *indicates significant ($P<0.05$) difference relative to values before rosiglitazone treatment. #indicates significant ($P<0.05$) differences between daily food intake values after 5 day treatment with rosiglitazone treatments. \$ indicates significant ($P<0.05$) differences between 7 day treatment values.

f: GW9662 induces suppression of food intake in DIO animals fed a high fat diet. Left column indicates daily food intake at the beginning of treatment (day 0). Middle column shows mean food intake after 5 days treatment with GW9662. Right column indicates daily food intake after 7 days DW9662 treatment. Green bar graph on right indicates daily food intake of animals with 7 day GW9662 treatment with honokiol in the last 2 days of the 7 day treatment. *indicates significant ($P<0.05$) difference relative to values before GW9662 treatment. #indicates significant ($P<0.05$) differences between daily food intake values after 5 day treatment with GW9662 treatments. \$ indicates significant ($P<0.05$) differences between 7 day treatment values.

g: 2 days icv. H2O2 treatment alone resulted in significantly ($P<0.05$) decreased daily food intake of DIO animals compared to vehicle treated controls.

h: Photomicrographs of pStat3 (red; asterisks) and POMC double immuno-labeled hypothalamic sections from leptin treated DIO mice co-treated with vehicle or H2O2 after peripheral leptin injections. There was significantly ($P<0.05$) higher percentage of POMC neurons with pStat3 labeled nucleus (arrow) in the arcuate nucleus of H2O2 treated mice compared to vehicle-treated controls. Bar scale represents 100 μm for both panels.